© 2016. Published by The Company of Biologists Ltd | Journal of Cell Science (2016) 129, 483-491 doi:10.1242/jcs.175976

RESEARCH ARTICLE

Activation of the IGF1 pathway mediates changes in cellular contractility and motility in single-suture craniosynostosis

Zeinab Al-Rekabi[1,2], Marsha M. Wheeler[3], Andrea Leonard[1], Adriane M. Fura[4], Ilsa Juhlin[1], Christopher Frazar[3], Joshua D. Smith[3], Sarah S. Park[2], Jennifer A. Gustafson[2], Christine M. Clarke[2], Michael L. Cunningham[2,5] and Nathan J. Sniadecki[1,4,*]

ABSTRACT

Insulin growth factor 1 (IGF1) is a major anabolic signal that is essential during skeletal development, cellular adhesion and migration. Recent transcriptomic studies have shown that there is an upregulation in IGF1 expression in calvarial osteoblasts derived from patients with single-suture craniosynostosis (SSC). Upregulation of the IGF1 signaling pathway is known to induce increased expression of a set of osteogenic markers that previously have been shown to be correlated with contractility and migration. Although the IGF1 signaling pathway has been implicated in SSC, a correlation between IGF1, contractility and migration has not yet been investigated. Here, we examined the effect of IGF1 activation in inducing cellular contractility and migration in SSC osteoblasts using micropost arrays and time-lapse microscopy. We observed that the contractile forces and migration speeds of SSC osteoblasts correlated with IGF1 expression. Moreover, both contractility and migration of SSC osteoblasts were directly affected by the interaction of IGF1 with IGF1 receptor (IGF1R). Our results suggest that IGF1 activity can provide valuable insight for phenotype–genotype correlation in SSC osteoblasts and might provide a target for therapeutic intervention.

KEY WORDS: Traction force, Cell migration, IGF1, IGF1R, Calvarial osteoblast, Single-suture craniosynostosis

INTRODUCTION

Insulin growth factor 1 (IGF1) is known to play a crucial role in both embryonic and postnatal skeletal development (Tahimic et al., 2013). *In vivo*, IGF1 signaling stimulates osteoblast survival, proliferation, differentiation and matrix production (Bodine et al., 2007; Guntur and Rosen, 2013). Osteoblasts express the IGF1 receptor (IGF1R) and secrete IGF1 into the microenvironment. In these cells, IGF1R mutations and IGF1 overexpression are found to correlate with skeletal and craniofacial defects (Cunningham et al., 2011; Guntur and Rosen, 2013). A lack of IGF1 and IGF1R in mutant mice results in severe retardation in bone development, hypomineralized skeletons and growth plate defects (Woods et al., 1996; Bikle et al., 2001). Therefore, IGF1 appears to act as a ubiquitous anabolic signal, playing an important role in bone development.

[1]Department of Mechanical Engineering, University of Washington, Seattle, WA 98195, USA. [2]Seattle Children's Research Institute, Center for Developmental Biology and Regenerative Medicine, Seattle, WA 98101, USA. [3]Department of Genome Sciences, University of Washington, Seattle, WA 98105, USA. [4]Department of Bioengineering, University of Washington, Seattle, WA 98105, USA. [5]Division of Craniofacial Medicine and the Department of Pediatrics, University of Washington, Seattle, WA 98105, USA.

*Author for correspondence (nsniadec@uw.edu)

Received 17 June 2015; Accepted 6 December 2015

It is becoming increasingly evident that there is a relationship between IGF1 signaling and the mechanobiology of osteoblasts (Laviola et al., 2007). Previous studies have implicated increased production of IGF1 in osteoblasts after mechanical loading (Reijnders et al., 2007; Klein-Nulend et al., 2013). IGF1 is also thought to be involved in stimulating other tissues, including skin, neurons and skeletal muscle cells, through its ability to induce cell migration (Guvakova, 2007). In particular, stimulating tissue-engineered muscles with IGF1 has been found to increase their contractility by promoting their differentiation, hypertrophy and force transmission (Gawlitta et al., 2008; Vandenburgh et al., 2008). In addition, IGF1 induces adhesion to extracellular matrix (ECM) proteins, suggesting that this pathway triggers the activation of integrins (Doerr and Jones, 1996; Manes et al., 1999). Moreover, IGF1 also appears to promote the association of the IGF1R to focal adhesion proteins, leading to increased cellular migration and invasion (Manes et al., 1999).

A number of pathological processes have been linked to the IGF1 pathway. Recently, the IGF1 signaling pathway has been implicated in the developmental pathology of craniosynostosis, which is defined as the premature fusion of calvarial bones (Stamper et al., 2012). Craniosynostosis divides into syndromic and non-syndromic forms, with syndromic forms defined as those with recognizable patterns of craniofacial and non-craniofacial malformations. A number of mutations are associated with syndromic craniosynostosis (Fitzpatrick, 2013; Sharma et al., 2013; Twigg et al., 2013; Twigg and Wilkie, 2015). However, the biological basis for the majority of cases of non-syndromic single-suture craniosynostosis (SSC) remains unknown. Recent work has shown that SSC is likely caused by contributions from both genetic and environmental factors, including maternal smoking (Kallen, 1999; Honein and Rasmussen, 2000), thyroid disease (Rasmussen et al., 2007; Carmichael et al., 2015a,b), fertility treatments (Reefhuis et al., 2003) and intrauterine head constraint (Graham et al., 1979, 1980; Graham and Smith, 1980). IGF1 and IGF1R are known to be expressed in the developing cranial sutures, where their interaction regulates bone growth, and their expression increases in response to strain forces (Roth et al., 1997; Bradley et al., 1999; Hirukawa et al., 2005). Furthermore, exogenous IGF1 has been found to induce increased expression of osteogenic markers in cranial sutures (Chen et al., 2003). The expression levels of these markers have been shown to be positively correlated with contractility and migration (Liaw et al., 1994; Kilian et al., 2010; Hunter et al., 2012; Wang et al., 2012). However, a correlation between IGF1 expression, osteoblast contractility and migration has not yet been investigated. Expanding our understanding of the biophysical factors underlying the pathogenesis of SSC might provide deeper insights into the processes involved in the earlier stages of this disease.

Journal of Cell Science (2016) 129, 483-491 doi:10.1242/jcs.175976

In this study, we hypothesize that calvarial osteoblasts derived from patients with SSC have increased contractility through activation of the IGF1 signaling pathway. Our findings demonstrate that increased expression of IGF1 in SSC osteoblasts or the addition of exogenous IGF1 correlates with larger contractile forces and reduced migration speeds as compared to control osteoblasts. Selectively inhibiting IGF1R in SSC osteoblasts resulted in a reduction of their traction forces, while their migration speeds appeared to increase. Our results reveal a relationship between IGF1 signaling, contractility and migration in SSC osteoblasts. We propose that the elevated levels of IGF1 expression observed in SSC patients might affect the mechanobiology of osteoblasts.

RESULTS

IGF1 expression in SSC osteoblasts

Primary osteoblast cell lines were developed from individuals diagnosed with SSC (cases, n=199) and from individuals who underwent cranial surgery but without a bone-related disease (controls, n=50). Transcriptomic analysis with microarrays was used to assess for differences in a transcript–transcript correlation structure (i.e. connectivity) between cases and controls. The differential connectivity test identified significant differences between transcripts involved in the IGF1 signaling pathway (P<0.05). Based on levels of IGF1 expression, we selected 15 cases and nine controls spanning from the highest IGF1 expression in cases (9.39) and controls (7.70) to the lowest that was similar for both cases and controls (5.29 for cases and 5.37 for controls) (Fig. S1A). Subsequently, the pattern of IGF1 expressions in these cells was assessed using high-throughput RNA sequencing (Fig. S1B). Levels of IGF1 expression on average were found to be higher in cases we selected as compared to the controls (P<0.05).

To assess whether the differentiation and proliferation of SSC and control osteoblasts correlated with IGF1 expression, we examined their alkaline phosphatase (ALP) activity and BrdU incorporation. SSC osteoblasts exhibited an increase in ALP activity compared to the controls (Fig. 1A). Although the average ALP activity appeared higher in SSC osteoblasts, the 95% confidence ellipses for both cases and controls overlapped (P>0.05). However, the ellipse surrounding the ALP activity in SSC osteoblast suggested a weak positive correlation to IGF1 expression (R-value=0.397) (Fig. 1B). Conversely, we found that the BrdU incorporation by SSC osteoblasts was significantly reduced compared to the controls (P=0.015) (Fig. 1C). Although the average BrdU incorporation appeared significantly lower in SSC osteoblasts, the 95% confidence ellipse for BrdU incorporation demonstrated a marginally weak negative correlation between proliferation and IGF1 expression in SSC osteoblasts (R-value=−0.029), which was not present in the controls (Fig. 1D). When taken together, our findings suggest that increased IGF1 expression might be associated with reduced BrdU incorporation (proliferation) and increased ALP activity (differentiation) in SSC osteoblasts.

Increased contractility is observed in SSC osteoblasts

To examine the effect of the IGF1 pathway on SSC osteoblast contractility, we seeded control (Fig. 2A) and SSC osteoblasts (Fig. 2B) onto micropost arrays, which were microcontact printed with fibronectin. The traction forces of the cells were measured by analyzing the deflections of the microposts using fluorescence microscopy and image analysis code (Han et al., 2012). SSC osteoblasts had similar morphologies as compared to the controls, but generated larger traction forces on the microposts (Fig. 2A,B).

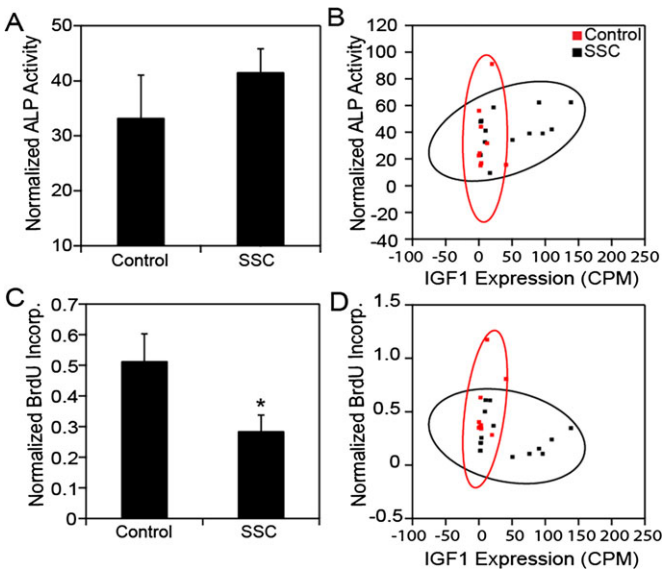

Fig. 1. IGF1 expression in SSC osteoblasts. The selected 15 SSC cases and nine controls were assessed for ALP expression (marker of differentiation) and BrdU incorporation (marker of proliferation). (A) SSC osteoblasts exhibited an increase in ALP activity compared to the controls; however, it was not statistically significant (P>0.05). (B) Plot of ALP expression as a function of IGF1 expression for both SSC osteoblasts and controls reveal overlapping 95% confidence ellipses. However, the ellipse surrounding ALP expressions of SSC osteoblasts suggested a weak positive correlation with increasing IGF1 expression (R-value=0.397). (C) BrdU incorporation by SSC osteoblasts was found to be significantly reduced as compared to the controls (P=0.015). (D) This result was also corroborated by the 95% ellipse surrounding the BrdU incorporation in SSC osteoblast, where a marginally weak negative correlation was found between proliferation and IGF1 expression (R-value=−0.029). Data shown as mean±s.e.m. from three experimental replicates. *P<0.05 (Student's t-test). P-values for the 95% confidence ellipses were determined by Spearman–Rank correlations.

To determine whether cell spreading is linked to the IGF1 pathway, the area of SSC and control osteoblasts on the microposts were analyzed by segmentation and thresholding. We found no significant difference in cell area between cases and controls (P=0.439) (Fig. 2C). However, when using a 95% confidence ellipse, we found a weak positive correlation between cell area and IGF1 expression for SSC (R-value=0.257), but this correlation was not observed for the controls (Fig. 2D).

Next, we examined whether cellular contractility in SSC was affected by IGF1 expression. We found that SSC osteoblasts produced significantly larger traction forces than the controls (P=1.17×10^{-4}), (Fig. 2E). Moreover, the confidence ellipse surrounding the traction force data for SSC osteoblasts demonstrated a positive correlation with IGF1 expression (R-value=0.532), and again, this correlation was not present in the controls (Fig. 2F). Thus, our findings implicate IGF1 as a factor in regulating the contractility of SSC osteoblasts. In examining whether SSC contractility is confounded by other factors such as sex or synostosis type (Figs S3 and S4), we found IGF1 expression to correlate with traction forces in a manner that was independent of sex or synostosis type.

Reduced migration is observed in SSC osteoblasts

Osteoblast migration has previously been demonstrated to be an important factor in the patterned growth of calvarial bones, where its impairment was found to lead to craniosynostosis in mouse models (Ting et al., 2009). To investigate the effect of the IGF1 pathway on the migration of SSC osteoblasts, we used a cell-tracking assay with

Journal of Cell Science (2016) 129, 483-491 doi:10.1242/jcs.175976

time-lapse microscopy over a 15-h period to trace the migration paths of cases and controls (Fig. 3A,B). Care was taken to track the centroid of the nucleus of migrating cells (Kim et al., 2014). The phase-contrast images overlaid with the migration tracks shown in Fig. 3A,B are representative of the cell populations examined, demonstrating that SSC osteoblasts migrate less than controls. Collecting the migration tracks for all cells analyzed on a rose plot, we observed that over a 15-h period, SSC osteoblasts migrated a shorter distance from their starting point (Fig. 3C,D). Furthermore, these cells moved at a significantly lower migration speed compared to the non-diseased osteoblasts (P=1.15×10^{-3}) (Fig. 3E). In comparing the 95% confidence ellipses surrounding the migration data, a negative correlation was observed in SSC osteoblasts (R-value=−0.486), which was not found in controls (Fig. 3F). This finding suggests that although IFG1 expression inhibits the migration of SSC osteoblasts, it might not be the only contributing factor to SSC. In addition, the length of the migration path was found to be significantly shorter for the cases (P=0.002) (Fig. S4A). These cells, unlike like the controls, showed a negative correlation to IGF1 expression (R-value=−0.396) (Fig. S4B). In addition, their displacement (Fig. S4D) and directionality (Fig. S4F) were also found to demonstrate a negative correlation to IGF1 expression compared to the controls (P<0.05), even though we observed no changes in their displacements (Fig. S4C) and directionality (Fig. S4E) (P<0.05). Taken together, our results provide strong evidence that IGF1 expression inhibits the migration of SSC osteoblasts.

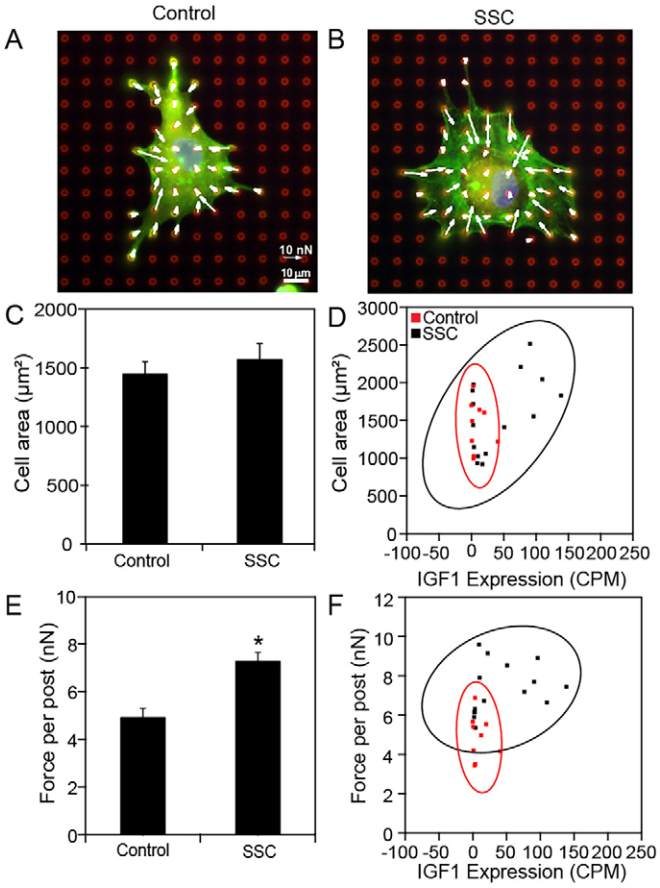

Fig. 2. Increased contractility observed in SSC osteoblasts. Representative fluorescent images and traction forces of a fixed and stained (A) control and (B) SSC osteoblast cells. Red, microposts; green, actin; blue, RUNX2 nuclear signal. Traction forces were measured by analyzing the deflections of the microposts and are reported as force vectors (arrows). (C) Cell spread area remained unchanged for SSC osteoblasts and controls (P=0.439). (D) A plot of the cell area as a function of IGF1 expression for both SSC osteoblasts and controls revealed overlapping 95% confidence ellipses; however, a weak positive correlation of cell area with IGF1 expression was observed for SSC (R-value=0.257). (E) The traction forces of SSC osteoblasts appeared significantly more contractile than the controls (P=1.17×10^{-4}). (F) The 95% confidence ellipse surrounding the traction forces of SSC osteoblasts demonstrated a positive correlation with IGF1 expression compared to the controls (R-value=0.532), suggesting that IGF1 is an important factor related to the disease. Data shown as mean±s.e.m. from three experimental replicates (Table S2). *P<0.05 (Student's t-test). P-values for the 95% confidence ellipses were determined by Spearman–Rank correlations.

IGF1R regulates osteoblast contractility and migration

From our RNA sequencing data, we identified over a thousand genes that significantly correlated with SSC osteoblast contractility and/or migration (Tables S3 and S4). The noteworthy targets we identified include *FGFR3*, *TGFBR1*, *TGFB3*, *WNT3*, *WNT5B*, *WNT16*, *CTBP2*, *DTX4*, *DVL2* and *ITGB1*, all of which have been implicated previously in bone development (Coussens et al., 2008; Yen et al., 2010; Brunner et al., 2011; Lories et al., 2013). Therefore, to ascertain whether IGF1 expression has a direct influence on osteoblast contractility and migration, we performed a deterministic study using exogenous IGF1 and a selective IGF1R inhibitor (NVP). We chose to compare two cell lines: the control osteoblast line with the lowest expression of IGF1 (Fig. 4A) and a SSC osteoblast line with the highest IGF1 expression (Fig. 4B). For the control osteoblasts, we found there was a significant increase in traction forces when these cells were stimulated with exogenous IGF1 (P=0.006) (Fig. 4A). Traction forces were not affected by the addition of NVP. However, the addition of exogenous IGF1 did counteract this increase. Following this, we considered the downstream effector myosin-II, which has previously been shown to play a major role in mechanotransduction by governing actomyosin contractility (Jaalouk and Lammerding, 2009; Buxboim et al., 2010). Inhibiting myosin-II ATPase activity with blebbistatin is well known to decrease traction forces relative to untreated cells (Beningo et al., 2006; Gardel et al., 2008). We found that treating the control osteoblasts with blebbistatin did not decrease their traction forces. However, control osteoblasts treated with both exogenous IGF1 and blebbistatin had traction forces that were not different to those of the untreated controls. These results indicate that exogenous IGF1 can cause an increase in cellular contractility.

Next, we examined the effect of exogenous IGF1, NVP and blebbistatin on SSC osteoblasts. Without any treatments, SSC osteoblasts were more contractile than the control cells. After stimulating SSC osteoblasts with exogenous IGF1, we found a significant increase in their traction forces as compared to the untreated conditions (P=0.012). After inhibiting IGF1R with NVP, we observed a significant loss in their force transmission (P=6.30×10^{-4}). Furthermore, we found no significant increase in force when cells treated with NVP were subsequently treated with exogenous IGF1. Their traction forces were notably lower in magnitude than untreated SSC osteoblasts (P=0.003). In addition, we also observed a significant loss in traction forces as a result of the treatment of SSC osteoblasts with blebbistatin (P=8.08×10^{-5}). When these blebbistatin-treated cells were subsequently treated with exogenous IGF1, we found a significant increase in force (P=0.029). This increase, although modest was still significantly lower than the forces produced by untreated SSC osteoblasts (P=2.06×10^{-4}). These results indicate that IGF1 regulates SSC osteoblast contractility through IGF1R.

Journal of Cell Science (2016) 129, 483-491 doi:10.1242/jcs.175976

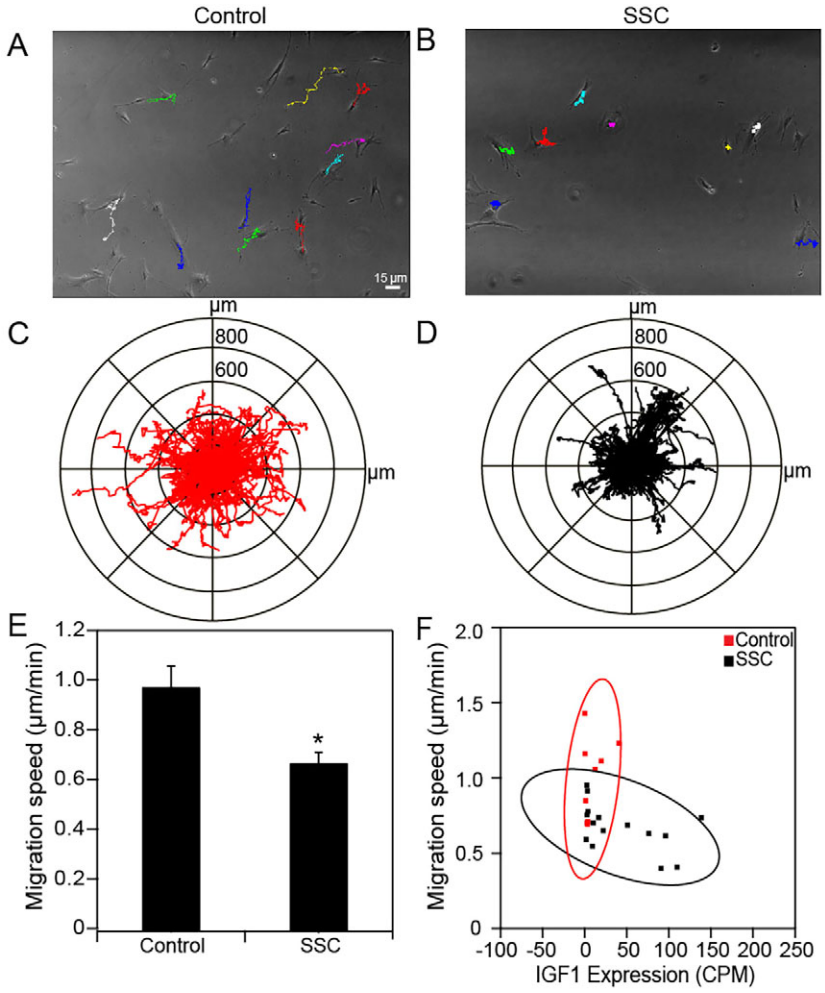

Fig. 3. Reduced migration observed in SSC osteoblasts. Time-lapse phase-contrast movies were obtained to observe the migration of (A) control and (B) SSC osteoblasts. Representative phase-contrast images were overlaid with the migration tracking data, where each color trace represents the path of a cell. Collecting the migration data for (C) controls and (D) SSC osteoblasts revealed that the controls explore a wider territory than SSC osteoblasts. (E) In addition, the migration speed was considerably reduced amongst SSC osteoblasts as compared to controls (P=1.15×10^{-3}). (F) When comparing the migration speeds of the select SSC and control osteoblasts to IGF1 expression, the 95% confidence ellipse surrounding the SSC osteoblasts showed a negative correlation to IGF1 expression in SSC osteoblasts (R-value=−0.486). Data shown as mean±s.e.m. from three experimental replicates (Table S2). *P<0.05 (Student's t-test). P-values for the 95% confidence ellipses were determined by Spearman–Rank correlations.

To examine the role of IGF1R in regulating osteoblast migration, we tracked both SSC and control osteoblasts over a 15-h period. Untreated controls appeared migratory (Fig. 5A). However, after stimulating these cells with exogenous IGF1, we found a significant loss in migration speed as compared to the untreated controls (P=0.017). Following this, we treated the cells with NVP or blebbistatin, and found that both of these treatments caused the controls to increase their migration speeds. The migration speeds of controls under both these treatments showed no change from the untreated controls. In observing SSC osteoblasts, these cells showed a significantly lower migration speed as compared to the controls (Fig. 5B). Treating these cells with exogenous IGF1 did not lead to a change in their migration speed. Conversely, supplementing the SSC osteoblasts with NVP or blebbistatin caused the cells to be more migratory as compared to their untreated counterparts (P=0.009 or P=0.001, respectively) (Fig. 5B). Furthermore, when these cells were given exogenous IGF1 stimulation, we found no effect on their migration speeds; however, this increase still remained significantly higher than the migration speed of untreated SSC osteoblasts (P=0.037 or P=7.62×10^{-4}, respectively). These findings demonstrate that IGF1R signaling regulates osteoblast migration.

DISCUSSION

This study examined the effect of IGF1 signaling in the mechanobiology of SSC osteoblasts. Herein, we demonstrated that the IGF1 signaling pathway affects SSC osteoblast contractility and migration. Mutations and/or overexpression in IGF1 and IGF1R has been associated with SSC and also results in growth retardation in both humans and mice (Baker et al., 1993; Liu et al., 1993; Woods et al., 1996; Cunningham et al., 2011). Recently, transcriptomic analysis has identified differential gene expression in both SSC osteoblasts and controls (Stamper et al., 2011). Furthermore, these differences in the correlation structure of the transcriptome have shown upregulation of IGF1 activity in calvarial SSC osteoblasts (Stamper et al., 2011). In this study, SSC osteoblasts with elevated IGF1 expression were observed to have higher traction forces than controls. SSC osteoblasts moved considerably slower, with shorter migration tracks, and thus reduced migration speeds. In contrast, inhibition of IGF1R and myosin-II caused a loss in traction force and an increase in migration speed, suggesting that SSC osteoblast contractility and migration might be regulated through the interaction of IGF1 and IGF1R.

Based on previous studies, it appears that the relationship between IGF1 and both cellular contractility and migration is dependent on the cell type. In a previous study, MCF-7 cells migrated in response to IGF1, but not in its absence (Manes et al., 1999). However, these cells also showed increased cellular adhesion because of an increase in FAK activity upon the presence of IGF1 (Manes et al., 1999). Furthermore, IGF1 has been found to induce contractility in retinal pigment epithelial cells (Mukherjee and Guidry, 2007) and muscle cells (Cvetkovic et al., 2014). These studies demonstrate that cells are likely to possess a response to IGF1 that is specific to the cell type.

Journal of Cell Science (2016) 129, 483-491 doi:10.1242/jcs.175976

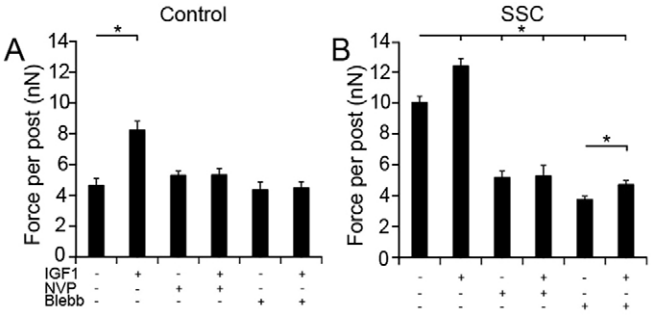

Fig. 4. IGF1R regulates osteoblast contractility. A control osteoblast line with the lowest expression of IGF1 and a SSC osteoblast line with the highest IGF1 expression were chosen for studying the role of IGF1 signaling on traction force. (A) Controls with low IGF1 expression appeared significantly more contractile upon stimulation with exogenous IGF1 (population size of experimental repetition, n_1=13, n_2=9, n_3=12; P=0.006) as compared to their untreated controls (n_1=14, n_2=3, n_3=10). Selectively inhibiting IGF1R (with NVP) (n_1=12, n_2=9, n_3=10) or myosin-II ATPase (with blebbistatin, Blebb) (n_1=12, n_2=9, n_3=11) did not affect traction forces. Stimulating NVP-treated (n_1=9, n_2=13, n_3=19), or blebbistatin-treated cells (n_1=12, n_2=10, n_3=9), with exogenous IGF1 resulted in no change in traction force. (B) Compared to the untreated SSC cells (population size of experimental repetition, n_1=10, n_2=12, n_3=11), SSC osteoblasts stimulated with IGF1 showed a significant increase in traction forces (n_1=9, n_2=14, n_3=9; P=0.012). When selectively inhibiting IGF1R, a loss in traction forces was observed (n_1=11, n_2=10, n_3=16; P=6.30×10^{-4}). NVP-treated cells subsequently treated with exogenous IGF1 remained unchanged compared to the NVP-treated cells; however, their traction forces were significantly lower than those of untreated SSC osteoblasts (P=0.003). Blebbistatin also caused the traction forces of SSC osteoblasts to be significantly reduced (n_1=12, n_2=12, n_3=9; P=8.08×10^{-5}). Stimulating the blebbistatin-treated SSC osteoblasts with exogenous IGF1 resulted in a small but significant increase in force (n_1=13, n_2=13, n_3=8; P=0.029); however, this increase still remained significantly lower than the forces of untreated SSC osteoblasts (P=2.06×10^{-4}). Data shown as mean±s.e.m. from three experimental replicates. *P<0.05 (one-way ANOVA with a Bonferroni's and Fischer post-hoc adjustment).

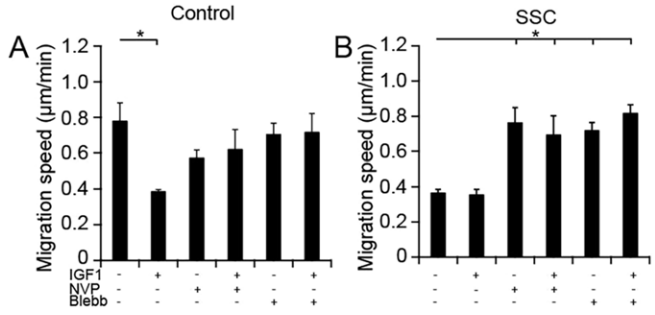

Fig. 5. IGF1R regulates osteoblast migration. A control osteoblast line with the lowest expression of IGF1 and a SSC osteoblast line with the highest IGF1 expression were chosen for studying the role of IGF1 signaling on migration. (A) Controls with low IGF1 expression appeared significantly less migratory upon IGF1 stimulation (population size of experimental repetition, $n_{1,2,3}$=3; P=0.017) compared to their untreated controls ($n_{1,2,3}$=3). Upon selectively inhibiting IGF1R (with NVP) ($n_{1,2,3}$=3) or myosin-II ATPase (with blebbistatin, Blebb) ($n_{1,2,3}$=3), the cells remained migratory. Furthermore, even after supplementing NVP-treated (n_1=2, $n_{2,3}$=3), or blebbistatin-treated cells ($n_{1,2,3}$=3) with exogenous IGF1, these cells still remained migratory. (B) Untreated SSC cells (n_1=4, n_2=3, n_3=2) and those stimulated with exogenous IGF1 (n_1=4, n_2=4, n_3=3) showed a decrease in migration speed as compared to untreated controls. When selectively inhibiting IGF1R, these cells were more migratory (n_1=3, n_2=2, n_3=4; P=0.009). Stimulating with IGF1 (n_1=4, n_2=4, n_3=3) did not lead to a further increase in migration; however, this increase still remained significantly higher to the migration speed of untreated SSC osteoblasts (P=0.037). Upon inhibiting myosin-II ATPase with blebbistatin ($n_{1,2,3}$=4), their migration speeds appeared significantly greater than the untreated SSC osteoblasts (P=0.001), even after IGF1 stimulation (n_1=4, n_2=3, n_3=4; P=7.62×10^{-4}). Data shown as mean±s.e.m. from three experimental replicates. *P<0.05 (one-way ANOVA with a Bonferroni's and Fischer post-hoc adjustment).

IGF1 is known to induce osteogenic markers, where its impact can be amplified as a result of the specific mechanobiology of osteoblasts. In particular, IGFI has been shown to induce the production of osteogenic markers including osteocalcin, osteopontin, alkaline phosphatase and type I collagen (Chen et al., 2003). In osteoblasts differentiated from mesenchymal stems cells, the expression of these same markers has been shown to increase in response to mechanical factors like applied strain (Rath et al., 2008), substrate stiffness (Engler et al., 2006) and cell shape (McBeath et al., 2004; Kilian et al., 2010). Moreover, it has been observed *in vivo* that a strain regimen applied to the tibia of transgenic mice overexpressing IGF1 in their osteoblasts leads to a five-fold increase in bone formation as compared to wild-type mice (Gross et al., 2002). Traction forces are an essential factor for the mechanotransduction of applied strain, substrate stiffness and cell shape (Ingber, 2006; Sniadecki et al., 2007; Chen, 2008; Buxboim et al., 2010; Al-Rekabi and Pelling, 2013). These studies highlight the importance of IGF1 activity in the mechanobiology of osteoblasts. Here, we have demonstrated that increased IGF1 expression and exogenous IGF1 induce an increase in cellular contractility in SSC osteoblasts. Therefore, it might be that increased contractility in SSC osteoblasts plays a synergistic role with IGF1 signaling in promoting osteogenesis.

Using pharmacological inhibitors of IGF1R and myosin-II ATPase, we found that the combined activity of IGF1 and IGF1R is sufficient to regulate cellular contractility. IGF1 binds to IGF1R, resulting in the autophosphorylation of this receptor (Taya et al., 2001). This autophosphorylation leads to the activation of various IGF1-dependent signal transductions (Taya et al., 2001) forming a complex with leukemia-associated Rho guanine nucleotide exchange factor (LARG, encoded by *ARHGEF12*) (Taya et al., 2001). LARG activates the Rho family GTPases, which are known to influence cytoskeletal remodeling and cell adhesion. Rho participates in the regulation of various cellular functions including stress fiber, focal adhesion formation (Chrzanowska-Wodnicka and Burridge, 1996), muscle contraction (Fukata et al., 2001) and membrane ruffling (Kurokawa and Matsuda, 2005). When considering the effect of NVP or blebbistatin treatment on the traction forces and migration speeds of SSC osteoblasts and controls, our findings suggest that IGF1 regulates osteoblast contractility and migration through its interaction with IGF1R and presumably involving the family of Rho GTPases, such as RhoA and Rac.

IGF1 has previously been shown to regulate keratinocyte shape by stimulating plasma membrane protrusion and spreading (Haase et al., 2003). Consistent with that study, we found a positive correlation between IGF1 expression and the cell area of SSC osteoblasts, supporting the idea that IGF1 influences cell spreading. Although we have previously observed an inverse relationship between traction forces per post and cell area (Han et al., 2012), this phenomenon was not observed in SSC osteoblasts. This behavior might be explained by the specific cell type responses, or by the fact that levels of IGF1 expression might trigger the Rho pathway, leading to cellular contractility, while also inducing Rac activity, promoting cell spreading in SSC osteoblasts.

The mechanism leading to the patterned growth of calvarial bones still remains elusive; however, this type of growth depends on the close regulation of osteoblast proliferation, differentiation and

Journal of Cell Science (2016) 129, 483-491 doi:10.1242/jcs.175976

migration (Hall and Miyake, 2000; Olsen et al., 2000). Recent work has shown that migration of calvarial osteoblasts plays a crucial role in the patterned growth of calvarial bones, where any abnormal migration of these cells can lead to the development of craniosynostosis (Ting et al., 2009). Considering the migration of osteoblasts derived from SSC individuals with elevated IGF1 activity, there appears to be a significant decrease in migration speeds relative to controls. This suggests that IGF1 influences migration and contributes to the development of SSC. In our previous study (Stamper et al., 2011), we demonstrated that differential IGF1 signaling results in upregulation of ECM-mediated focal adhesions. Moreover, IGF1 signaling has also been implicated in mediating focal adhesion formation and cell migration (Manes et al., 1999; Andersson et al., 2009).

In previous literature, the role of androgen and estrogen signaling has been implicated in the promotion of osteogenesis (James et al., 2009; Lin et al., 2007). Sex-based differences have been used in characterizing transcriptional changes identified in SSC patients (Stamper et al., 2012; Park et al., 2015). One particular work used mouse models to evaluate the role of estrogens in suture fusion (James et al., 2009), finding that estrogens promoted osteoblast differentiation (James et al., 2009). Moreover, another study found that dihydrotesterone induced expression of osteogenic markers leading to sagittal synostosis in mice (Lin et al., 2007). In contrast to these results, our study found no relationship between sex or synostosis type with IGF1 expression in either SSC osteoblasts or controls (Figs S2 and S3). This could be due to our limited sampling size (15 SSC osteoblasts and nine controls) or to the fact that the IGF1 signaling pathway is a ubiquitous anabolic signal that is independent of sex or synostosis type (Tahimic et al., 2013).

Our findings support the role of IGF1 as a key factor in the pathogenesis of SSC. Moreover, our data interpretation also provides some evidence that lower levels of IGF1 (<50 CPM reads) might combine with other growth factors, which have previously been associated to the development of SSC. Indeed, the interplay between IGF1 and Wnt or Fgf signaling pathways has been suggested to contribute to the pathogenesis of craniosynostosis (ten Berge et al., 2008; Behr et al., 2010; Maruyama et al., 2010). For example, a number of mutations, including in the *FGFR3*, *TGFBR1* and *TGFB3* genes, have been associated with syndromic forms of the disease (Passos-Bueno et al., 2008; Cunningham et al., 2011). The Notch signaling pathway has also been linked to craniosynostosis as a result of its association with tissue boundary formation, which is important during the patterned growth of the skull (Yen et al., 2010). Additionally, a microarray study has identified upregulation of Wnt signaling in tissues (Miraoui et al., 2010), and other studies have identified *WNT5B* expression in post-natal growth plates (Andrade et al., 2007) and *WNT16* as suppressing osteoblast differentiation in craniofacial bone formation (Jiang et al., 2014). Here, we used correlation analysis to investigate whether these transcripts are associated with SSC. Here, we found that *FGFR3*, *TGFBR1*, *TGFB3*, *WNT3*, *WNT5B*, *WNT16*, *CTBP2*, *DTX4* and *DVL2* are correlated to contractility and/or migration in SSC osteoblasts (Tables S3 and S4). These findings suggest that there is an interplay between the IGF1 pathway and the aforementioned transcripts, which might act in an integrative manner leading to the development of SSC. Nevertheless, our inhibition studies indicate that enhanced signaling through the IGF1 pathway is crucial to the contractility–migration phenotype observed in SSC in a manner that is independent of the role of these other factors.

Previous studies have found an upregulation of ECM components and matrix mineralization in craniosynostosis (Lomri et al., 1998; Lemonnier et al., 2001), and another study has found the majority of genes related to cell adhesion and ECM composition to be downregulated (Fanganiello et al., 2007). Here, we found no correlation between integrins and contractility in SSC osteoblasts, although we observed a significant correlation between *ITGB1* and migration in SSC osteoblasts (Tables S3 and S4). Therefore, future studies are necessary in order to clarify the precise mechanism that integrates all the mechanotransduction pathways associated to SSC.

Our findings imply that IGF1 activation mediates changes in cellular contractility and migration in SSC osteoblasts. The exact mechanism leading to the development of SSC appears to be highly complex and is not entirely understood at present. Our results provide supporting evidence that IGF1 is one of the important signaling factors associated with SSC and might act through mechanotransduction mechanisms associated with traction forces and migration. Further investigation of the IGF1 signaling pathway will provide deeper insights into the mechanisms that regulate the development of SSC and might be useful in the development of diagnostic and treatment strategies.

MATERIALS AND METHODS

Ethics statement

For all subjects with SSC, informed consent was obtained. All samples were obtained according to the principles expressed in the Declaration of Helsinki. A waiver of consent was obtained from the Seattle Children's Hospital's Institutional Review Board (IRB) for the use of anonymous control samples. Given that our study is Health Insurance Portability and Accountability Act (HIPAA) compliant, independent prospective Institutional Review Board (IRB) approval was obtained from each of the institutions providing bone samples including Seattle Children's Hospital, Northwestern University in Chicago, Children's Health Care of Atlanta, and St. Louis Children's Hospital.

Participant enrollment

As previously described (Stamper et al., 2011; Park et al., 2015), 84% of the eligible cases approached for consent were enrolled in the study. Computed tomography (CT) scans identified and confirmed isolated sagittal, coronal, metopic or lambdoid synostosis. The exclusion criteria involved the presence of major serious medical or neurological conditions, such as syndromic craniosynostosis, cardiac defects, seizure disorders, cerebral palsy and other significant health conditions requiring surgical corrections or the presence of three or more minor or major extra-cranial malformations. The control samples in this study were obtained from patients undergoing cranial surgery for reasons other than craniosynostosis (e.g. hydrocephalus or brain tumor) or autopsies. Control samples did not include patients with skeletal dysplasias, due to the possibility of any confounding effects caused by the mechanobiology of other bone-related diseases.

Cell culture

As previously described (Stamper et al., 2011; Park et al., 2015), harvested calvaria samples were obtained from individuals undergoing surgery for sagittal, coronal, metopic or lambdoid synostosis (Fig. S1C,D and Table S1). Infants were referred to the study at the time of diagnosis by their treating surgeon or pediatrician and were eligible if, at the time of enrollment, the CT scans identified and confirmed isolated sagittal, coronal, metopic or lambdoid synostosis. Briefly, calvaria samples from craniosynostosis cases were obtained from discarded tissues during surgical reconstructive procedures, whereas control calvaria samples were obtained from discarded tissues from anonymous surgical or autopsy specimens. These samples were then washed with Waymouth medium (Sigma-Aldrich) and cleaned of all soft tissue. They were then sliced into thin 3–5-mm diameter pieces and placed in 12-well plates. As the osteoblasts reached confluency, the contents of each 12-well place were

Journal of Cell Science (2016) 129, 483-491 doi:10.1242/jcs.175976

trypsinized using 0.05% Trypsin (Gibco Life Technologies) and passaged into T75 flasks. After reaching confluence, the samples were frozen in liquid nitrogen in 90% fetal bovine serum (Gibco Life Technologies) and 10% DMSO (Fisher Scientific). SSC and control osteoblast cell lines were grown from cryogenic vials and cultured in T25 flasks containing Waymouth's medium supplemented with 10% fetal bovine serum (Hyclone Laboratories) and 1% streptomycin-penicillin (Hyclone Laboratories) in a 37°C, 5% CO_2 incubator. Cells were harvested at 70% confluency for RNA isolation.

TruSeq stranded mRNA preparation

Next-generation sequencing libraries were prepared from 1.25 µg of total RNA in an automated, high-throughput format using the TruSeq Stranded mRNA kit (Illumina). All the steps required for library construction were automated and performed on a Sciclone NGSx Workstation (Perkin Elmer). For library construction, ribosomal RNA was depleted by means of a poly-A enrichment and first- and second-strand cDNA syntheses were subsequently performed. Each library was then uniquely barcoded using the Illumina adapters and amplified using a total of 13 cycles of PCR. After amplification and PCR cleanup, library concentrations were quantified using the Quant-it dsDNA Assay (Life Technologies). Libraries were subsequently normalized and pooled based on Agilent 2100 Bioanalyzer results (Agilent Technologies). Pooled libraries were size selected using a Pippin Prep (Sage Science) and then balanced by mass and pooled in batches of 96, with a final pool concentration of 2–3 nM, for sequencing on a HiSeq 4000 machine.

Read processing and analysis pipeline

RNA sequence reads were aligned to the human genome (hg19) with the reference transcriptome from Ensemble v67 using Tophat (Kim et al., 2013). In the resulting alignment files, duplicate reads were marked using the Picard MarkDuplicates tool (http://broadinstitute.github.io/picard/), then local realignment was performed around indels, and base quality score recalibration was run using GATK tools (McKenna et al., 2010). Aligned reads mapping to genes were quantified with HTseq (http://www-huber.embl.de/HTSeq/doc/overview.html) and converted into count per million (CPM) read values using R software (Dataset GSE75524).

Microarray processing

RNA extraction, assessment, analysis and quality control were carried out as previously described (Dataset GSE27976; Stamper et al., 2011; Park et al., 2015). In brief, the selected cell lines were thawed and cultured in T25 flasks. At 75% confluence, the cells were passaged to a density of 1.75×10^5 cells per 25 cm^2 and subjected to RNA extraction using the Roche High Pure miRNA Isolation Kit (Roche) according to the manufacturer's instructions. RNA integrity was assessed using an Agilent 2100 Bioanalyzer with only samples passing quality control run on Affymetrx Human Gene 1.0 ST arrays on which 28,869 genes are represented. The raw microarray data was further analyzed with Bioconductor (Gentleman et al., 2004) and normalized RMA method as implemented by the Bioconductor affy package.

ALP and BrdU proliferation assays

For the ALP assay, 1.5×10^4 cells/cm^2 were plated in 96-well dishes. At 48 h after seeding the cells, the medium was removed and cells were rinsed with PBS (Corning). Next, 0.2 ml p-nitrophenyl phosphate (pNPP; Sigma-Aldrich) was added to the wells and incubated in the dark for 1 h at room temperature. After incubation, 0.05 ml of 3 M NaOH was added to each well to stop the reaction and the samples were analyzed on a SpectraMAX 190 spectrophotometer (Molecular Devices) at the 405-nm wavelength. Finally, to assess the proliferation rates, BrdU incorporation was measured using the BrdU Cell Proliferation kit (EMD Millipore). At 24 h after cell plating (1.5×10^4 cells/cm^2 were plated in 96-well dishes), 1× BrdU reagent diluted with Waymouth's medium was added to the wells and incubated for 24 h. The assay was carried out according to the manufacturer's protocol.

Inhibitions and stimulation

For the inhibition and stimulation experiments, cells grown to a cell density of ~10^5 cells/cm^2 in six-well dishes were serum-starved in 0.1% FBS (Life Technologies) for 4 h prior to adding the treatments. IGF1 (EMD Millipore), blebbistatin (Sigma-Aldrich) and NVP-AEW541 (Cayman Chemical) were stored as stock solutions in DMSO or sterile, deionized water. Inhibition of myosin-II ATPase or IGF1R was achieved by exposing cells to 15 µM blebbistatin for 30 min or 0.16 µM NVP-AEW541 for 20 min, respectively. In some cases, cells were stimulated with 35 ng/ml IGF1 for 15 min along with blebbistatin or NVP-AEW541 treatment.

Micropost preparation, staining and imaging

After 24 h, the controls and SSC osteoblast cells were plated on arrays of microposts and fibronectin-coated (50 µg/ml, Corning) six-well culture dishes with a cell density of ~10^5 cells/cm^2. Arrays of 9-µm-spaced polydimethylsiloxane (PDMS; Dow-Corning) microposts were fabricated on top of glass coverslips through a replica-molding process (Sniadecki and Chen, 2007), using a mixing ratio of 10:1 for the base and curing agent for 6 h at 110°C. SSC and control osteoblasts were attached on top of the microposts through microcontact printing fibronectin (50 µg/ml, Corning) onto the tips of these posts (Sniadecki and Chen, 2007). After stamping, the arrays were immersed in 2 µg/ml bovine serum albumin (BSA)-conjugated Alexa Fluor 594 (Molecular Probes) for 1 h to stain the PDMS so that the posts could be observed with fluorescent microscopy. After staining, the arrays were submerged in 0.2% Pluronic F-127 solution (Sigma-Aldrich) for 30 min to block the adsorption of additional proteins to the surface of the microposts. Cells were seeded onto the micropost arrays and allowed to attach for 2 h. Afterwards, unattached cells were washed away with additional medium, and the remaining cells on the microposts were cultured overnight. Cells on the microposts were fixed with 4% paraformaldehyde and permeabilized with 0.5% Triton X-100. Cells were then quenched in 0.15 M glycine for 25 min. Actin filaments were stained with Alexa-Fluor-488-conjugated phalloidin (Molecular Probes), and the nuclei stained with anti-RUNX2 antibody conjugated to Dylight 488 (NBP1-77461G, Novus Biologicals), a direct osteogenic marker of osteoblast lineage cells. Imaging was carried out on an epi-fluorescent microscope (Nikon TEi; Nikon, Instruments) with a 40× oil objective (NA 1.00).

Force and migration measurements

Given that microposts can be analyzed as cantilever beams, the deflection (δ) of a micropost was used to determine the traction force (F) of a cell according to $F=k\delta=(3\pi ED^4/64L^2)\,\delta$, where E is the Young's modulus of PDMS, D is the diameter of the post, and L is the post height (Sniadecki and Chen, 2007). Each micropost had a height of 8 µm, diameter of 2.1 µm, and spring constant of k=16.6 nN/µm, resulting in an effective shear modulus of 1.7 MPa. For the aspect ratio of the micropost (L/D=3.9), a correction factor k_{tilt}=0.81, in which $F=k_{tilt}k\delta$, was included in the calculation to account for tilting at the compliant base of the microposts (Schoen et al., 2010). Images obtained from epi-fluorescence microscopy were analyzed with custom-built codes in MATLAB (MathWorks; available from the corresponding author) to measure the deflection of each micropost underneath a cell as well as the spread area of the cell. The total traction force per cell, F_{tot} was calculated as $\Sigma_{i=1}^{n_{post}} F_i$, where F_i is the force at each micropost and n_{post} is the number of microposts beneath a given cell. In an effort to compare traction forces irrespective of cell area (Han et al., 2012), we reported the traction forces as the force per post (F_{tot}/n_{post}). For migration experiments, cells were cultured in six-well dishes coated with fibronectin and imaged every 5 min during a period of 15 h using time-lapse phase-contrast microscopy on an inverted microscopy (Nikon TEi) with a 4× air objective (NA 0.13) in a 37°C, 5% CO_2 chamber. An ImageJ plugin (MTrackJ) was used to track the nucleus of the individual cells.

Statistical analysis

Data were obtained from three replicates (n_1, n_2, n_3) for each of the 15 cases and nine controls (Table S2). All values are presented as the mean±s.e.m. Samples were analyzed for significance using either a Student's t-test or a one-way ANOVA with a Bonferroni's and Fischer post-hoc adjustment. Comparisons were considered significant for $P<0.05$ (marked with asterisks in the figures). In some cases, 95% confidence ellipses (regions that statistically enclose 95% of the data points) were used as visual guides to examine the correlation of the

data to IGF1 expression. Furthermore, for statistical correlation analysis of the transcriptome level versus force or migration, Spearman–Rank correlations were performed on the data. Only the transcripts with $P<0.05$ are listed in Tables S3 and S4.

Competing interests

The authors declare that N.J.S. is a co-founder and has equity in Stasys Medical Corporation.

Author contributions

Z.A.-R., M.L.C. and N.J.S. conceived and designed the experiments. Z.A.-R., A.L., C.F., J.D.S., S.S.P. and J.A.G. performed the experiments. Z.A.-R., M.M.W., A.L., A.M.F., I.J., S.S.P., M.L.C. and N.J.S. analyzed the data. Z.A.-R., M.M.W., A.L., C.F., J.D.S., S.S.P., J.A.G. and C.M.C. contributed reagents, materials and/or analysis tools. Z.A.-R., M.L.C. and N.J.S. wrote the paper.

Funding

This work was supported by the National Institutes of Health (NIH), National Institute of Dental and Craniofacial Research (NIDCR) [grant number R01DE018227 to M.L.C., N.J.S.]; the Jean Renny Endowment for Craniofacial Research (to M.L.C.), and an National Science Foundation (NSF) CAREER award (to N.J.S.). Deposited in PMC for release after 12 months.

Supplementary information

Supplementary information available online at
http://jcs.biologists.org/lookup/suppl/doi:10.1242/jcs.175976/-/DC1

References

Al-Rekabi, Z. and Pelling, A. E. (2013). Cross talk between matrix elasticity and mechanical force regulates myoblast traction dynamics. *Phys. Biol.* **10**, 066003.
Andersson, S., D'Arcy, P., Larsson, O. and Sehat, B. (2009). Focal adhesion kinase (FAK) activates and stabilizes IGF-1 receptor. *Biochem. Biophys. Res. Commun.* **387**, 36-41.
Andrade, A. C., Nilsson, O., Barnes, K. M. and Baron, J. (2007). Wnt gene expression in the post-natal growth plate: regulation with chondrocyte differentiation. *Bone* **40**, 1361-1369.
Baker, J., Liu, J.-P., Robertson, E. J. and Efstratiadis, A. (1993). Role of insulin-like growth factors in embryonic and postnatal growth. *Cell* **75**, 73-82.
Behr, B., Longaker, M. T. and Quarto, N. (2010). Differential activation of canonical Wnt signaling determines cranial sutures fate: a novel mechanism for sagittal suture craniosynostosis. *Dev. Biol.* **344**, 922-940.
Beningo, K. A., Hamao, K., Dembo, M., Wang, Y.-L. and Hosoya, H. (2006). Traction forces of fibroblasts are regulated by the Rho-dependent kinase but not by the myosin light chain kinase. *Arch. Biochem. Biophys.* **456**, 224-231.
Bikle, D., Majumdar, S., Laib, A., Powell-Braxton, L., Rosen, C., Beamer, W., Nauman, E., Leary, C. and Halloran, B. (2001). The skeletal structure of insulin-like growth factor I-deficient mice. *J. Bone Miner. Res.* **16**, 2320-2329.
Bodine, P. V. N., Seestaller-Wehr, L., Kharode, Y. P., Bex, F. J. and Komm, B. S. (2007). Bone anabolic effects of parathyroid hormone are blunted by deletion of the Wnt antagonist secreted frizzled-related protein-1. *J. Cell. Physiol.* **210**, 352-357.
Bradley, J. P., Han, V. K. M., Roth, D. A., Levine, J. P., McCarthy, J. G. and Longaker, M. T. (1999). Increased IGF-I and IGF-II mRNA and IGF-I peptide in fusing rat cranial sutures suggest evidence for a paracrine role of insulin-like growth factors in suture fusion. *Plast. Reconstr. Surg.* **104**, 129-138.
Brunner, M., Millon-Fremillon, A., Chevalier, G., Nakchbandi, I. A., Mosher, D., Block, M. R., Albiges-Rizo, C. and Bouvard, D. (2011). Osteoblast mineralization requires beta1 integrin/ICAP-1-dependent fibronectin deposition. *J. Cell Biol.* **194**, 307-322.
Buxboim, A., Rajagopal, K., Brown, A. E. X. and Discher, D. E. (2010). How deeply cells feel: methods for thin gels. *J. Phys. Condens. Matter* **22**, 194116.
Carmichael, S. L., Clarke, C. M. and Cunningham, M. L. (2015a). Craniosynostosis: the potential contribution of thyroid-related mechanisms. *Curr. Epidemiol. Rep.* **2**, 1-7.
Carmichael, S. L., Ma, C., Rasmussen, S. A., Cunningham, M. L., Browne, M. L., Dosiou, C., Lammer, E. J. and Shaw, G. M. (2015b). Craniosynostosis and risk factors related to thyroid dysfunction. *Am. J. Med. Genet. A* **167**, 701-707.
Chen, C. S. (2008). Mechanotransduction - a field pulling together? *J. Cell Sci.* **121**, 3285-3292.
Chen, Y., Zhang, D. S., Tao, P. Y., Xu, P., Feng, S. Z., Mu, X. Z. and Wei, M. (2003). The effect of insulin-like growth factor 1 on the fusion of cranial suture. *Zhonghua Zheng Xing Wai Ke Za Zhi* **19**, 11-14.
Chrzanowska-Wodnicka, M. and Burridge, K. (1996). Rho-stimulated contractility drives the formation of stress fibers and focal adhesions. *J. Cell Biol.* **133**, 1403-1415.
Coussens, A. K., Hughes, I. P., Wilkinson, C. R., Morris, C. P., Anderson, P. J., Powell, B. C. and van Daal, A. (2008). Identification of genes differentially expressed by prematurely fused human sutures using a novel in vivo - in vitro approach. *Differentiation* **76**, 531-545.
Cunningham, M. L., Horst, J. A., Rieder, M. J., Hing, A. V., Stanaway, I. B., Park, S. S., Samudrala, R. and Speltz, M. L. (2011). IGF1R variants associated with isolated single suture craniosynostosis. *Am. J. Med. Genet. A* **155**, 91-97.
Cvetkovic, C., Raman, R., Chan, V., Williams, B. J., Tolish, M., Bajaj, P., Sakar, M. S., Asada, H. H., Saif, M. T. A. and Bashir, R. (2014). Three-dimensionally printed biological machines powered by skeletal muscle. *Proc. Natl. Acad. Sci. USA* **111**, 10125-10130.
Doerr, M. E. and Jones, J. I. (1996). The roles of integrins and extracellular matrix proteins in the insulin-like growth factor I-stimulated chemotaxis of human breast cancer cells. *J. Biol. Chem.* **271**, 2443-2447.
Engler, A. J., Sen, S., Sweeney, H. L. and Discher, D. E. (2006). Matrix elasticity directs stem cell lineage specification. *Cell* **126**, 677-689.
Fanganiello, R. D., Sertie, A. L., Reis, E. M., Yeh, E., Oliveira, N. A., Bueno, D. F., Kerkis, I., Alonso, N., Cavalheiro, S., Matsushita, H. et al. (2007). Apert p. Ser252Trp mutation in FGFR2 alters osteogenic potential and gene expression of cranial periosteal cells. *Mol. Med.* **13**, 422-442.
Fitzpatrick, D. R. (2013). Filling in the gaps in cranial suture biology. *Nat. Genet.* **45**, 231-232.
Fukata, Y., Kaibuchi, K., Amano, M. and Kaibuchi, K. (2001). Rho-Rho-kinase pathway in smooth muscle contraction and cytoskeletal reorganization of non-muscle cells. *Trends Pharmacol. Sci.* **22**, 32-39.
Gardel, M. L., Sabass, B., Ji, L., Danuser, G., Schwarz, U. S. and Waterman, C. M. (2008). Traction stress in focal adhesions correlates biphasically with actin retrograde flow speed. *J. Cell Biol.* **183**, 999-1005.
Gawlitta, D., Boonen, K. J. M., Oomens, C. W. J., Baaijens, F. P. T. and Bouten, C. V. C. (2008). The influence of serum-free culture conditions on skeletal muscle differentiation in a tissue-engineered model. *Tissue Eng. A* **14**, 161-171.
Gentleman, R. C., Carey, V. J., Bates, D. M., Bolstad, B., Dettling, M., Dudoit, S., Ellis, B., Gautier, L., Ge, Y., Gentry, J. et al. (2004). Bioconductor: open software development for computational biology and bioinformatics. *Genome Biol.* **5**, R80.
Graham, J. M., Jr and Smith, D. W. (1980). Metopic craniostenosis as a consequence of fetal head constraint: two interesting experiments of nature. *Pediatrics* **65**, 1000-1002.
Graham, J. M., Jr, deSaxe, M. and Smith, D. W. (1979). Sagittal craniostenosis: fetal head constraint as one possible cause. *J. Pediatr.* **95**, 747-750.
Graham, J. M., Jr, Badura, R. J. and Smith, D. W. (1980). Coronal craniostenosis: fetal head constraint as one possible cause. *Pediatrics* **65**, 995-999.
Gross, T. S., Srinivasan, S., Liu, C. C., Clemens, T. L. and Bain, S. D. (2002). Noninvasive loading of the murine tibia: an in vivo model for the study of mechanotransduction. *J. Bone Miner. Res.* **17**, 493-501.
Guntur, A. R. and Rosen, C. J. (2013). IGF-1 regulation of key signaling pathways in bone. *BoneKEy Rep.* **2**, 437.
Guvakova, M. A. (2007). Insulin-like growth factors control cell migration in health and disease. *Int. J. Biochem. Cell Biol.* **39**, 890-909.
Haase, I., Evans, R., Pofahl, R. and Watt, F. M. (2003). Regulation of keratinocyte shape, migration and wound epithelialization by IGF-1- and EGF-dependent signalling pathways. *J. Cell Sci.* **116**, 3227-3238.
Hall, B. K. and Miyake, T. (2000). All for one and one for all: condensations and the initiation of skeletal development. *BioEssays* **22**, 138-147.
Han, S. J., Bielawski, K. S., Ting, L. H., Rodriguez, M. L. and Sniadecki, N. J. (2012). Decoupling substrate stiffness, spread area, and micropost density: a close spatial relationship between traction forces and focal adhesions. *Biophys. J.* **103**, 640-648.
Hirukawa, K., Miyazawa, K., Maeda, H., Kameyama, Y., Goto, S. and Togari, A. (2005). Effect of tensile force on the expression of IGF-I and IGF-I receptor in the organ-cultured rat cranial suture. *Arch. Oral Biol.* **50**, 367-372.
Honein, M. A. and Rasmussen, S. A. (2000). Further evidence for an association between maternal smoking and craniosynostosis. *Teratology* **62**, 145-146.
Hunter, C., Bond, J., Kuo, P. C., Selim, M. A. and Levinson, H. (2012). The role of osteopontin and osteopontin aptamer (OPN-R3) in fibroblast activity. *J. Surg. Res.* **176**, 348-358.
Ingber, D. E. (2006). Cellular mechanotransduction: putting all the pieces together again. *FASEB J.* **20**, 811-827.
Jaalouk, D. E. and Lammerding, J. (2009). Mechanotransduction gone awry. *Nat. Rev. Mol. Cell Biol.* **10**, 63-73.
James, A. W., Theologis, A. A., Brugmann, S. A., Xu, Y., Carre, A. L., Leucht, P., Hamilton, K., Korach, K. S. and Longaker, M. T. (2009). Estrogen/estrogen receptor alpha signaling in mouse posterofrontal cranial suture fusion. *PLoS ONE* **4**, e7120.
Jiang, Z., Von den Hoff, J. W., Torensma, R., Meng, L. and Bian, Z. (2014). Wnt16 is involved in intramembranous ossification and suppresses osteoblast differentiation through the Wnt/beta-catenin pathway. *J. Cell. Physiol.* **229**, 384-392.
Kallen, K. (1999). Maternal smoking and craniosynostosis. *Teratology* **60**, 146-150.
Kilian, K. A., Bugarija, B., Lahn, B. T. and Mrksich, M. (2010). Geometric cues for directing the differentiation of mesenchymal stem cells. *Proc. Natl. Acad. Sci. USA* **107**, 4872-4877.

Kim, D., Pertea, G., Trapnell, C., Pimentel, H., Kelley, R. and Salzberg, S. L. (2013). TopHat2: accurate alignment of transcriptomes in the presence of insertions, deletions and gene fusions. *Genome Biol.* **14**, R36.
Kim, D.-H., Cho, S. and Wirtz, D. (2014). Tight coupling between nucleus and cell migration through the perinuclear actin cap. *J. Cell Sci.* **127**, 2528-2541.
Klein-Nulend, J., Bakker, A. D., Bacabac, R. G., Vatsa, A. and Weinbaum, S. (2013). Mechanosensation and transduction in osteocytes. *Bone* **54**, 182-190.
Kurokawa, K. and Matsuda, M. (2005). Localized RhoA activation as a requirement for the induction of membrane ruffling. *Mol. Biol. Cell* **16**, 4294-4303.
Laviola, L., Natalicchio, A. and Giorgino, F. (2007). The IGF-I signaling pathway. *Curr. Pharm. Des.* **13**, 663-669.
Lemonnier, J., Haÿ, E., Delannoy, P., Lomri, A., Modrowski, D., Caverzasio, J. and Marie, P. J. (2001). Role of N-cadherin and protein kinase C in osteoblast gene activation induced by the S252W fibroblast growth factor receptor 2 mutation in Apert craniosynostosis. *J. Bone Miner. Res.* **16**, 832-845.
Liaw, L., Almeida, M., Hart, C. E., Schwartz, S. M. and Giachelli, C. M. (1994). Osteopontin promotes vascular cell adhesion and spreading and is chemotactic for smooth muscle cells in vitro. *Circ. Res.* **74**, 214-224.
Lin, I. C., Slemp, A. E., Hwang, C., Sena-Esteves, M., Nah, H.-D. and Kirschner, R. E. (2007). Dihydrotestosterone stimulates proliferation and differentiation of fetal calvarial osteoblasts and dural cells and induces cranial suture fusion. *Plast. Reconstr. Surg.* **120**, 1137-1147.
Liu, J.-P., Baker, J., Perkins, A. S., Robertson, E. J. and Efstratiadis, A. (1993). Mice carrying null mutations of the genes encoding insulin-like growth factor I (Igf-1) and type 1 IGF receptor (Igf1r). *Cell* **75**, 59-72.
Lomri, A., Lemonnier, J., Hott, M., de Parseval, N., Lajeunie, E., Munnich, A., Renier, D. and Marie, P. J. (1998). Increased calvaria cell differentiation and bone matrix formation induced by fibroblast growth factor receptor 2 mutations in Apert syndrome. *J. Clin. Invest.* **101**, 1310-1317.
Lories, R. J., Corr, M. and Lane, N. E. (2013). To Wnt or not to Wnt: the bone and joint health dilemma. *Nat. Rev. Rheumatol.* **9**, 328-339.
Manes, S., Mira, E., Gomez-Mouton, C., Zhao, Z. J., Lacalle, R. A. and Martinez-A, C. (1999). Concerted activity of tyrosine phosphatase SHP-2 and focal adhesion kinase in regulation of cell motility. *Mol. Cell. Biol.* **19**, 3125-3135.
Maruyama, T., Mirando, A. J., Deng, C. X. and Hsu, W. (2010). The balance of WNT and FGF signaling influences mesenchymal stem cell fate during skeletal development. *Sci. Signal.* **3**, ra40.
McBeath, R., Pirone, D. M., Nelson, C. M., Bhadriraju, K. and Chen, C. S. (2004). Cell shape, cytoskeletal tension, and RhoA regulate stem cell lineage commitment. *Dev. Cell* **6**, 483-495.
McKenna, A., Hanna, M., Banks, E., Sivachenko, A., Cibulskis, K., Kernytsky, A., Garimella, K., Altshuler, D., Gabriel, S., Daly, M. et al. (2010). The Genome Analysis Toolkit: a MapReduce framework for analyzing next-generation DNA sequencing data. *Genome Res.* **20**, 1297-1303.
Miraoui, H., Ringe, J., Haupl, T. and Marie, P. J. (2010). Increased EFG- and PDGFalpha-receptor signaling by mutant FGF-receptor 2 contributes to osteoblast dysfunction in Apert craniosynostosis. *Hum. Mol. Gen.* **19**, 1678-1689.
Mukherjee, S. and Guidry, C. (2007). The insulin-like growth factor system modulates retinal pigment epithelial cell tractional force generation. *Invest. Ophthalmol. Vis. Sci.* **48**, 1892-1899.
Olsen, B. R., Reginato, A. M. and Wang, W. (2000). Bone development. *Annu. Rev. Cell Dev. Biol.* **16**, 191-220.
Park, S. S., Beyer, R. P., Smyth, M. D., Clarke, C. M., Timms, A. E., Bammler, T. K., Stamper, B. D., Mecham, B. H., Gustafson, J. A. and Cunningham, M. L. (2015). Osteoblast differentiation profiles define sex specific gene expression patterns in craniosynostosis. *Bone* **76**, 169-176.
Passos-Bueno, M. R., Serti Eacute, A. E., Jehee, F. S., Fanganiello, R. and Yeh, E. (2008). Genetics of craniosynostosis: genes, syndromes, mutations and genotype-phenotype correlations. *Front. Oral Biol.* **12**, 107-143.
Rasmussen, S. A., Yazdy, M. M., Carmichael, S. L., Jamieson, D. J., Canfield, M. A. and Honein, M. A. (2007). Maternal thyroid disease as a risk factor for craniosynostosis. *Obstet. Gynecol.* **110**, 369-377.
Rath, B., Nam, J., Knobloch, T. J., Lannutti, J. J. and Agarwal, S. (2008). Compressive forces induce osteogenic gene expression in calvarial osteoblasts. *J. Biomech.* **41**, 1095-1103.
Reefhuis, J., Honein, M. A., Shaw, G. M. and Romitti, P. A. (2003). Fertility treatments and craniosynostosis: California, Georgia, and Iowa, 1993–1997. *Pediatrics* **111**, 1163-1166.
Reijnders, C. M. A., Bravenboer, N., Tromp, A. M., Blankenstein, M. A. and Lips, P. (2007). Effect of mechanical loading on insulin-like growth factor-I gene expression in rat tibia. *J. Endocrinol.* **192**, 131-140.
Roth, D. A., Gold, L. I., Han, V. K. M., McCarthy, J. G., Sung, J. J., Wisoff, J. H. and Longaker, M. T. (1997). Immunolocalization of transforming growth factor beta 1, beta 2, and beta 3 and insulin-like growth factor I in premature cranial suture fusion. *Plast. Reconstr. Surg.* **99**, 300-309; discussion 310-306.
Schoen, I., Hu, W., Klotzsch, E. and Vogel, V. (2010). Probing cellular traction forces by micropillar arrays: contribution of substrate warping to pillar deflection. *Nano Lett.* **10**, 1823-1830.
Sharma, V. P., Fenwick, A. L., Brockop, M. S., McGowan, S. J., Goos, J. A. C., Hoogeboom, A. J. M., Brady, A. F., Jeelani, N. O., Lynch, S. A., Mulliken, J. B. et al. (2013). Mutations in TCF12, encoding a basic helix-loop-helix partner of TWIST1, are a frequent cause of coronal craniosynostosis. *Nat. Genet.* **45**, 304-307.
Sniadecki, N. J. and Chen, C. S. (2007). Microfabricated silicone elastomeric post arrays for measuring traction forces of adherent cells. *Methods Cell Biol.* **83**, 313-328.
Sniadecki, N. J., Anguelouch, A., Yang, M. T., Lamb, C. M., Liu, Z., Kirschner, S. B., Liu, Y., Reich, D. H. and Chen, C. S. (2007). Magnetic microposts as an approach to apply forces to living cells. *Proc. Natl. Acad. Sci. USA* **104**, 14553-14558.
Stamper, B. D., Park, S. S., Beyer, R. P., Bammler, T. K., Farin, F. M., Mecham, B. and Cunningham, M. L. (2011). Differential expression of extracellular matrix-mediated pathways in single-suture craniosynostosis. *PLoS ONE* **6**, e26557.
Stamper, B. D., Mecham, B., Park, S. S., Wilkerson, H., Farin, F. M., Beyer, R. P., Bammler, T. K., Mangravite, L. M. and Cunningham, M. L. (2012). Transcriptome correlation analysis identifies two unique craniosynostosis subtypes associated with IRS1 activation. *Physiol. Genomics* **44**, 1154-1163.
Tahimic, C. G. T., Wang, Y. and Bikle, D. D. (2013). Anabolic effects of IGF-1 signaling on the skeleton. *Front. Endocrinol.* **4**, 6.
Taya, S., Inagaki, N., Sengiku, H., Makino, H., Iwamatsu, A., Urakawa, I., Nagao, K., Kataoka, S. and Kaibuchi, K. (2001). Direct interaction of insulin-like growth factor-1 receptor with leukemia-associated RhoGEF. *J. Cell Biol.* **155**, 809-820.
ten Berge, D., Brugmann, S. A., Helms, J. A. and Nusse, R. (2008). Wnt and FGF signals interact to coordinate growth with cell fate specification during limb development. *Development* **135**, 3247-3257.
Ting, M.-C., Wu, N. L., Roybal, P. G., Sun, J., Liu, L., Yen, Y. and Maxson, R. E., Jr (2009). EphA4 as an effector of Twist1 in the guidance of osteogenic precursor cells during calvarial bone growth and in craniosynostosis. *Development* **136**, 855-864.
Twigg, S. R. F. and Wilkie, A. O. M. (2015). A genetic-pathophysiological framework for craniosynostosis. *Am. J. Hum. Genet.* **97**, 359-377.
Twigg, S. R. F., Vorgia, E., McGowan, S. J., Peraki, I., Fenwick, A. L., Sharma, V. P., Allegra, M., Zaragkoulias, A., Sadighi Akha, E., Knight, S. J. L. et al. (2013). Reduced dosage of ERF causes complex craniosynostosis in humans and mice and links ERK1/2 signaling to regulation of osteogenesis. *Nat. Genet.* **45**, 308-313.
Vandenburgh, H., Shansky, J., Benesch-Lee, F., Barbata, V., Reid, J., Thorrez, L., Valentini, R. and Crawford, G. (2008). Drug-screening platform based on the contractility of tissue-engineered muscle. *Muscle Nerve* **37**, 438-447.
Wang, Y.-K., Yu, X., Cohen, D. M., Wozniak, M. A., Yang, M. T., Gao, L., Eyckmans, J. and Chen, C. S. (2012). Bone morphogenetic protein-2-induced signaling and osteogenesis is regulated by cell shape, RhoA/ROCK, and cytoskeletal tension. *Stem Cells Dev.* **21**, 1176-1186.
Woods, K. A., Camacho-Hübner, C., Savage, M. O. and Clark, A. J. L. (1996). Intrauterine growth retardation and postnatal growth failure associated with deletion of the insulin-like growth factor I gene. *N. Engl. J. Med.* **335**, 1363-1367.
Yen, H.-Y., Ting, M.-C. and Maxson, R. E. (2010). Jagged1 functions downstream of Twist1 in the specification of the coronal suture and the formation of a boundary between osteogenic and non-osteogenic cells. *Dev. Biol.* **347**, 258-270.